

*"I don't take this model seriously. I think it is a convenient way to remember the numbers."*

W.W. Shane in Discussion III.5

## THE KINEMATICS WITHIN M31

Morton S. Roberts, Robert N. Whitehurst,\* and Tom R. Cram  
National Radio Astronomy Observatory<sup>†</sup>  
Green Bank, West Virginia

Abstract A new hydrogen line survey of M31 is described. A rotation curve of the galaxy is derived from these data. The northern half of the rotation curve can be traced to 27 kpc, the southern to 30 kpc. They are in general agreement; both sides show an extensive region of essentially constant rotational velocity.

A high sensitivity 21-cm survey of M31 was made with the Effelsberg 100-m telescope over a region  $\sim 5^\circ \times 1.5^\circ$ . Velocity profiles were obtained at approximately 1400 positions spaced at half-beam (4!5) intervals. These data have been prepared in various formats for publication as a 21-cm catalogue of M31 (Cram, Roberts, and Whitehurst, in preparation) and include profiles,  $\ell$ - $v$  contour diagrams, and grey-scale displays. All of the data emphasize the inadequacy of a thin, flat disk model for M31. This is illustrated in Fig. 1, an  $\ell$ - $v$  contour diagram for a line parallel to the major axis but displaced 18' to the SE. The bifurcation is due to double-peaked profiles, one velocity component is due to planar HI, the other to HI extending out of the plane at a different radius and hence a different observed radial velocity. A single line of sight senses both HI features. The lower, less intense feature (at  $-\lambda$  values) is consistent with the rotation curve derived from major axis data.

Detailed modeling of the spatial (x,y,z) distribution of HI in M31 is discussed in the following paper. Here we derive the rotation curve for M31. The major axis is the only region for which this can be done unambiguously. There are two reasons for this: (1) radial motions (expansion or contraction) are not sensed on the major axis, the

\* On leave from the Department of Physics and Astronomy, the University of Alabama.

<sup>†</sup> Operated by Associated Universities, Inc., under contract with the National Science Foundation.

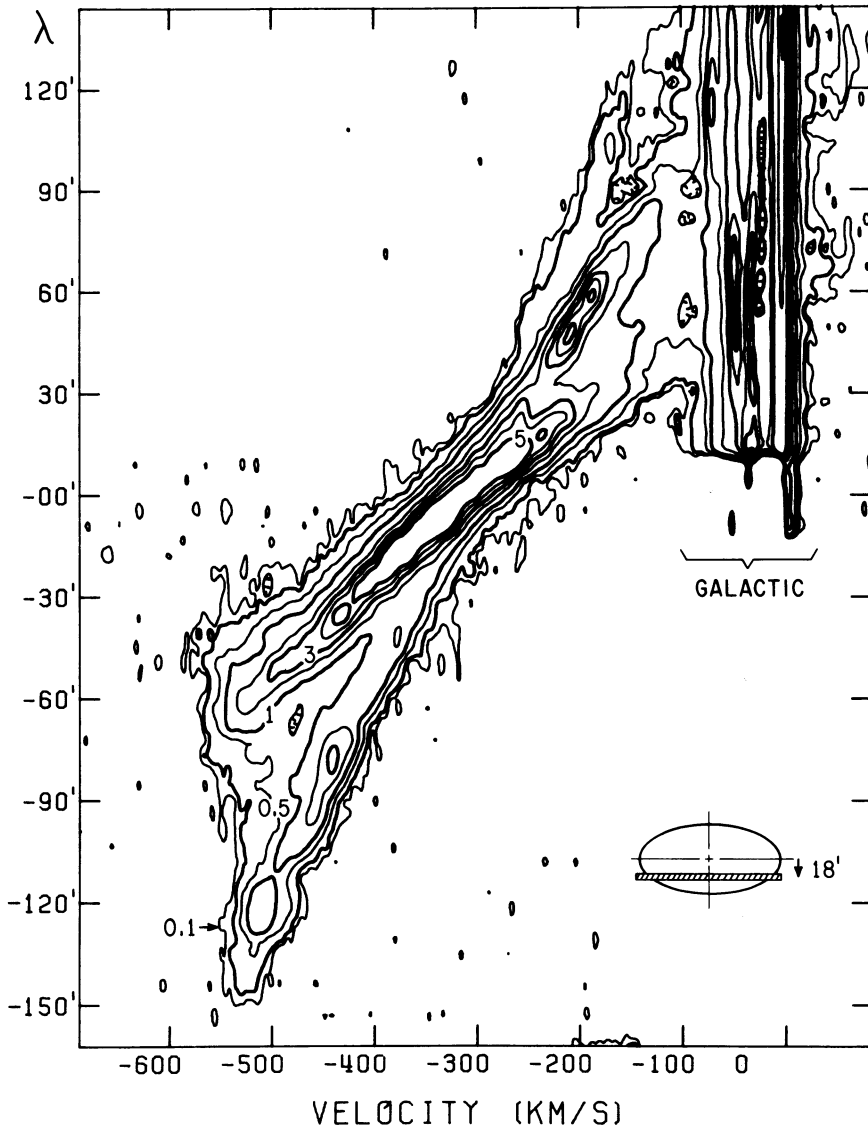


Fig. 1 - An  $\lambda$ - $v$  diagram for a line parallel to the major axis ( $\lambda$  axis) displaced  $18'$  to the SE, see the insert in the lower right. A thin disk model predicts a single diagonal feature rather than the bifurcation shown. Contour levels are from 0.1 to 5 K antenna temperature.

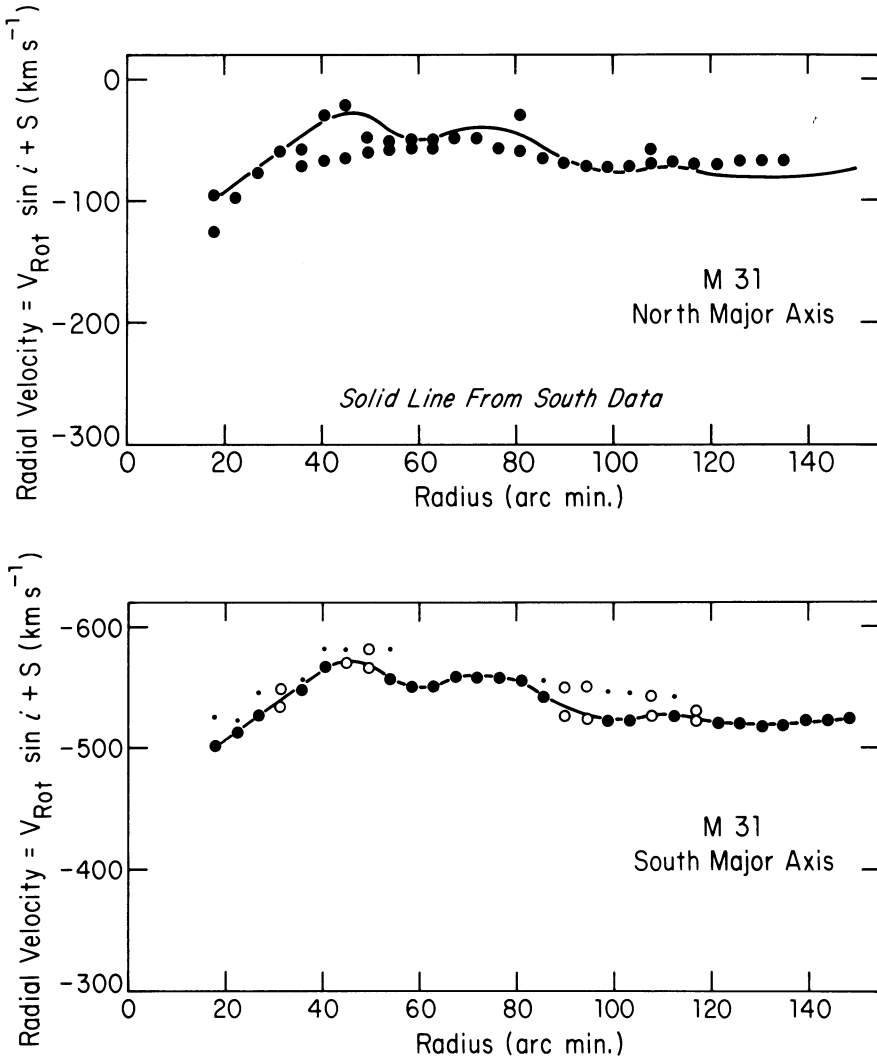


Fig. 2 - Rotation curve for M31 derived from major axis data. The upper panel is for the northern half of the Galaxy, the lower panel is for the southern half. The ordinate is observed radial velocity. At a distance of 690 kpc, 10' corresponds to 2 kpc. See the text for an explanation of the different symbols. The smoothly varying line is taken as the rotation curve of M31 and has been used for all modeling analysis.

projection yields Doppler velocities given by  $E(R) \sin i \sin \theta$ , where  $E(R)$  is the radial term and  $\theta$  is zero on the major axis. And (2), even though line of sight confusion may be present, features with radial velocities greater than the rotational velocity on the major axis,  $V_{\text{rot}} \sin i$ , cannot occur in a pure rotational model; or even one with moderate radial motions, except at large  $\theta$ .

Thus, for complex profiles on the major axis, which is generally the case for  $R \lesssim 100'$ , the problem becomes one of identifying the highest velocity feature present. This is accomplished by decomposing complex profiles into enough Gaussian components to yield a residual noise level in the profile region similar to that of the baseline region. Generally 4 to 6 components are necessary. The highest velocity component is identified as  $(V_{\text{rot}} \sin i)$ . The area under each component, i.e., the integrated brightness temperature, is not considered unless the highest velocity feature has an area less than a tenth of the next highest velocity feature. In these cases the peak velocity may be an artifact of the fitting procedures and is ignored in constructing the final rotation curve. Such weak features are retained in the display and are shown as small dots in Fig. 2 while the much stronger and next highest velocity feature is shown as a larger filled circle at the same radius. When two features are shown of similar velocity but differing by less than a factor of ten in their areas both are shown as open circles.

The northern half of the rotation curve, Fig. 2, is derived by a similar Gaussian-fitting procedure. But here Galactic foreground hydrogen is present and the approach of seeking the highest velocity component does not apply as easily. By studying the continuity of Galactic hydrogen in various  $\ell$ - $v$  displays a consistent set of data points are found--though, at times, two possible values are indicated. All values of  $(V_{\text{rot}} \sin i, R)$  are plotted in Fig. 2, including alternate choices at particular  $R$ 's. The rotation curve from the southern half is shown superposed (using a heliocentric systemic velocity of  $-300 \text{ km s}^{-1}$ ). The agreement, even to the ripples in the curve, between south and north is good, and we conclude that the same rotation curve applies to both halves of the galaxy. The rotation curve for  $R < 20'$  is not derived here. The motions in this region are clearly complex; contraction as well as a significant nonplanar component are suggested.

#### DISCUSSION FOLLOWING PAPER III.4 GIVEN BY M.S. ROBERTS

VAN WOERDEN: A sequence of double-peaked profiles like that shown by Dr. Roberts may, in principle, also be caused by gas in an infinitesimally thin disk. Consider two circular filaments of radii  $R_1 = 90'$  and  $R_2 = 110'$ , both having the same rotation speed  $V_c$ . With  $\cos i = 0.2$ , their separation will be less than  $5'$  over the range  $0' < x < 60'$  ( $x$  = coordinate along major axis), and both will be within the  $9'$  beam for  $y = 18'$  over this range of  $x$ . Observed velocities  $V_1, V_2$  are given by  $V_i = V_c \sin i x/R_i$ ; hence one beam will see two peaks whose separation

is proportional to  $x$ . The velocity separation exceeds the smearing caused by the extent of the beam in  $x$  for  $x > 40'$ .

M.S. ROBERTS: The highly idealized model van Woerden proposes will yield double-peaked profiles. However this model fails completely when one looks at the quantitative data, i.e. velocity separation of the peaks (up to 100 km/s), spatial extent, and signal strength.

SHANE: High resolution Westerbork HI data which will be discussed in a later contribution [see Discussion III.5] support the interpretation as given by Roberts.

COURTÈS: The problem of superposition on the major axis is maybe not so severe on the Andromeda nebula because of the large hole in the HI distribution. The inner HI arm for example is narrow and very far from the center of M31.

M.S. ROBERTS: Even on the major axis there is a wide spread of velocities of well over 100 km/s. You cannot explain this in terms of beam effects. Everything is consistent with a thick model.

LANDECKER: HI SURVEY OF M31

A survey of neutral hydrogen in the whole of M31 has been made with the Synthesis Telescope at Penticton, Canada. The field of view of the instrument is  $2^\circ$  and the synthesized beam is  $2' \times 3'$ . Low order spacings have been supplied from 25-m telescope observations. Velocity resolution is 5 km/s. The noise on line maps is 2 K r.m.s. and on the continuum map 0.1 K. M31 has been covered in 4 regions centered at  $\pm 45'$  and  $\pm 125'$  from the optical center.